J Biol Inorg Chem (2011) 16:1241–1254
DOI 10.1007/s00775-011-0812-9

ORIGINAL PAPER

The electron transfer complex between nitrous oxide reductase and its electron donors

Simone Dell'Acqua · Isabel Moura · José J. G. Moura · Sofia R. Pauleta

Received: 29 March 2011 / Accepted: 20 June 2011 / Published online: 8 July 2011

Abstract Identifying redox partners and the interaction surfaces is crucial for fully understanding electron flow in a respiratory chain. In this study, we focused on the interaction of nitrous oxide reductase (N_2OR), which catalyzes the final step in bacterial denitrification, with its physiological electron donor, either a *c*-type cytochrome or a type 1 copper protein. The comparison between the interaction of N_2OR from three different microorganisms, *Pseudomonas nautica*, *Paracoccus denitrificans*, and *Achromobacter cycloclastes*, with their physiological electron donors was performed through the analysis of the primary sequence alignment, electrostatic surface, and molecular docking simulations, using the bimolecular complex generation with global evaluation and ranking algorithm. The docking results were analyzed taking into account the experimental data, since the interaction is suggested to have either a hydrophobic nature, in the case of *P. nautica* N_2OR, or an electrostatic nature, in the case of *P. denitrificans* N_2OR and *A. cycloclastes* N_2OR. A set of well-conserved residues on the N_2OR surface were identified as being part of the electron transfer pathway from the redox partner to N_2OR (Ala495, Asp519, Val524, His566 and Leu568 numbered according to the *P. nautica* N_2OR sequence). Moreover, we built a model for *Wolinella succinogenes* N_2OR, an enzyme that has an additional *c*-type-heme-containing domain. The structures of the N_2OR domain and the *c*-type-heme-containing domain were modeled and the full-length structure was obtained by molecular docking simulation of these two domains. The orientation of the *c*-type-heme-containing domain relative to the N_2OR domain is similar to that found in the other electron transfer complexes.

Keywords Electron transfer complexes · Docking · Recognition · Nitrous oxide reductase · Electron transfer pathway

Introduction

Electron transfer reactions between proteins are essential for a large number of biological processes that include redox changes, such as some metabolic processes, photosynthesis, and both aerobic and anaerobic respiration. In most bacteria, the denitrification pathway is induced by low oxygen tensions or anaerobic conditions in the presence of nitrate and involves the reduction of nitrate to nitrogen (N_2) [1, 2]. This global conversion is catalyzed by a group of enzymes, nitrate reductases, nitrite reductases, nitric oxide reductases, and nitrous oxide reductases (N_2ORs), that contain transition metals as cofactors. The global process requires ten electrons that must be transferred stepwise to these enzymes through small electron donor proteins, such as *c*-type cytochromes or type 1 copper proteins, such as pseudoazurins and azurins [1, 2].

In general, electron transfer complexes are part of a group of protein–protein complexes, the transient complexes, that are characterized by a short lifetime (on the

Electronic supplementary material The online version of this article (doi:10.1007/s00775-011-0812-9) contains supplementary material, which is available to authorized users.

S. Dell'Acqua · I. Moura · J. J. G. Moura (✉) · S. R. Pauleta (✉)
REQUIMTE/CQFB,
Departamento de Química,
Faculdade de Ciências e Tecnologia,
Universidade Nova de Lisboa,
2829-516 Caparica, Portugal
e-mail: jose.moura@dq.fct.unl.pt

S. R. Pauleta
e-mail: srp@dq.fct.unl.pt

millisecond timescale) and a low binding affinity (K_d in the millimolar to micromolar range) [3, 4]. This transient nature distinguishes the electron transfer complexes from the more stable, long-lived protein–protein complexes, such as inhibitor–enzyme complexes, antigen–antibody complexes, and signal transduction complexes.

The transient nature of these complexes, necessary for a rapid electron transfer, makes them difficult to crystallize. As a consequence, only a few three-dimensional structures of complexes of this type have been determined by X-ray crystallography [5]. An alternative to the co-crystallization is offered by protein–protein docking simulations using the coordinates of the individual proteins, coupled with experimental data that provide information on the binding interface, such as mutagenesis studies and NMR chemical shift mapping.

Several docking algorithms have been developed [Attract, BiGGER, ClusPro, 3D-DOCK, DOT, Gramm-X, HADDOCK, ICM-DISCO, Molfit, PatchDock, RosettaDock, SKE-DOCK, Smooth-Dock, ZDOCK [6, and references therein], with HADDOCK and BiGGER being the ones mostly used to predict electron transfer complexes. In this study, we used bimolecular complex generation with global evaluation and ranking (BiGGER), which is included in the Chemera free software package [7].

BiGGER has been used in the last decade to obtain structural models of several electron transfer and protein–protein complexes [8–10], in most cases when the three-dimensional structures of the proteins involved are available and the residues at the interface are either not known or known only for one of the partners. Although the coordinates used are considered as "rigid bodies", the algorithm offers an option called "soft-docking" that takes into account the conformational freedom of some of the surface residue side chains, such as lysine, to assist the prediction of the mode of binding of the two proteins. However, for a complete analysis, the model structure of the complexes obtained needs to be validated by experimental data, such as from mutagenesis studies, kinetic studies of the electron transfer, or the identification of the interaction surface by chemical shift perturbation (using 2D NMR titrations).

In this work, the N_2OR from different species, which catalyzes the final step of the bacterial denitrification pathway, the two-electron reduction of nitrous oxide (N_2O) to dinitrogen (N_2) [2, 11], is used as a case study. The three-dimensional structures of N_2OR from *Pseudomonas nautica* [12], *Paracoccus denitrificans* [13], and *Achromobacter cycloclastes* [14] were solved recently, revealing the presence of two multicopper centers: a binuclear electron transfer center, CuA center, and a tetranuclear catalytic center, CuZ center. The large distance between the CuA and CuZ centers within the same monomer imposes the dimeric conformation of the enzyme, which is thus a functional homodimer, in which the two subunits are oriented "head to tail", bringing the CuA and CuZ centers to approximately 10 Å from each other, a distance appropriate for an efficient electron transfer [15].

The binuclear CuA center of N_2OR is located in a cupredoxin-like domain similar to that found in cytochrome *c* oxidase and which in both cases constitutes the proposed docking and electron entry site from the small electron donor and enables transfer to the catalytic center [11, 16, 17]. The CuZ center is located in the N-terminal domain, which adopts a seven-blade β-propeller fold.

Recently, the physiological electron donor of *P. nautica* N_2OR was identified to be cytochrome *c*-552 [18]. A steady-state kinetic study demonstrated that the interaction between the two proteins is mainly hydrophobic in nature and that mitochondrial cytochrome *c* is not a competent electron donor to this enzyme [18]. On the other hand, N_2OR isolated from *Paracoccus pantotrophus*, an organism closely related to *P. denitrificans*, can accept electrons from cytochrome *c*-550 and pseudoazurin [19–21], and also from the mitochondrial cytochrome *c* [22]. A structural model for the electron transfer complex between *P. denitrificans* N_2OR and either *P. panthotropus* cytochrome *c*-550 or *P. panthotropus* pseudoazurin has been proposed on the basis of a theoretical docking study [23]. In the case of *A. cycloclastes* N_2OR, its electron donor was shown to be only pseudoazurin [24], since no small cytochrome *c* was identified in the periplasm of the bacteria growing under denitrifying conditions [25]. Nevertheless, it was shown that bovine heart cytochrome *c* was also able to reduce the CuA center [26].

In *Wolinella succinogenes*, a host-associated organism from the *Epsilonproteobacteria* group, an N_2OR was identified and isolated that exhibits a unique structural feature with an additional C-terminal domain containing a *c*-type heme, which is not present in any other N_2OR that has been isolated [27]. This N_2OR receives electrons from a small periplasmic *c*-type cytochrome isolated from the same organism [28].

The purpose of this study was to analyze the electron transfer complexes formed between *P. nautica* N_2OR, *P. denitrificans* N_2OR, and *A. cycloclastes* N_2OR and their physiological electron donors using a molecular docking approach, and to compare the results obtained with those for the nonphysiological redox partners. The ab initio calculated docked solutions were filtered using the properties of the electron transfer complexes derived from the kinetic studies. The putative model structures are discussed in terms of selectivity of binding and the electron transfer pathway. Moreover, a model for *W. succinogenes* N_2OR was built and this structure was compared with the model structure of an electron transfer complex of a small *c*-type cytochrome docked to N_2OR.

Methods

Molecular docking simulation

Molecular docking simulations were performed using the algorithm BiGGER developed by Palma et al. [7]. The target protein was the functional dimer of N_2OR and the probes were each putative electron donor proteins. The coordinates for the *P. nautica* N_2OR (1QNI [12]), *P. denitrificans* N_2OR (1FWX [13]), *A. cycloclastes* N_2OR (2IWF [14]), *P. nautica* cytochrome *c*-552 (1CNO [29]), *P. denitrificans* cytochrome *c*-550 (1COT [30]), *P. panthotropus* pseudoazurin (3ERX [31]), *A. cycloclastes* pseudoazurin (1BQR (reduced) [32]), horse heart cytochrome *c* (1HRC [33]), and bovine heart cytochrome *c* (2B4Z [34]) were obtained from the RCSB Protein Data Bank (http://www.rcsb.org).

The BiGGER algorithm provides a complete and systematic search of the rotational space of one protein relative to the other, generating a large number of putative docking geometries based on the complementarity of the molecular surfaces. The 5,000 best generated solutions were evaluated and ranked according to a combination of additional interaction criteria that included electrostatic energy of interaction, relative solvation energy, and the relative propensity of side chains to interact. For each solution, this evaluation process produces a "global score". The solutions can also be ranked according to each individual criterion, such as the electrostatic score or the hydrophobic score. The top solutions were analyzed using PISA (http://www.ebi.ac.uk/msd-srv/prot_int/pistart.html) to determine the size of the interface area of the complex and its hydrophobicity.

Analysis of the electrostatic surface potential

The electrostatic potential of the small electron donor proteins used in this study was generated in Chimera using the Coulombic law and partial charges from the Amber 99SB force field for all residues except for hemes, where the charges were calculated by the Gasteiger method [35]. The electrostatic potential of N_2ORs used in this study was generated using the PDB2PQR server and the Adaptative Poisson–Boltzmann Solver plug-in in PyMOL (http://www.pymol.org).

Analysis of the electron transfer pathways

The donor–acceptor coupling constant and the most probable electron transfer pathway were predicted using the PATHWAYS algorithm [36, 37], which is included in the HARLEM molecular modeling program (http://www.kurnikov.org/harlem_manual/html/index.html). The electronic coupling matrix element (H_{AB}) depends strongly on the distance between the donor and the acceptor, since covalent bonds, and also hydrogen bonds to a lesser extent, produce a much stronger electronic coupling than a through-space connection [38].

Sequence analysis and alignment

Sequence alignment was carried out using the program ClustalW [39] on the EBI Web site. The WHISCY program [40] was used to predict the N_2OR residues involved in protein–protein interfaces. This program is based on sequence conservation and also takes into account structural information.

Model building for *W. succinogenes* N_2OR

The model of the N-terminal domain of *W. succinogenes* N_2OR was obtained through the Web-based Protein Homology/analogY Recognition Engine [41] (PHYRE; http://www.sbg.bio.ic.ac.uk/phyre/), whereas the C-terminal domain was modeled using both PHYRE and SWISS-MODEL [42]. Putative model structures of *W. succinogenes* N_2OR were predicted by analysis of the complexes obtained from the docking, performed with the BiGGER algorithm [7], between the model structure of the N_2OR domain and *c*-type-heme-containing domain.

Results and discussion

Surface homology analysis of partner proteins

N_2OR is a homodimer, with each monomer being composed of two domains. The N-terminal domain has a seven-blade β-propeller fold, which is named the catalytic domain, since it holds the CuZ center, whereas the C-terminal domain, containing the CuA center, has a cupredoxin fold and is the electron transferring domain. In Fig. 1a, c, and e, the structures of the three N_2OR used in this study (from *P. nautica*, *P. denitrificans*, and *A. cycloclastes*) are represented as backbones, evidencing their functional homodimeric structure, whereas in Fig. 1b, d, and f their surfaces are shown colored by electrostatic potential.

The comparison of the electrostatic surface of these N_2ORs reveals that the region around the CuA center, which is the proposed electron entry point, has a negative patch, which differs in size depending on the enzyme. In the case of *P. nautica* N_2OR, the electrostatic surface is the least negative, whereas *P. denitrificans* N_2OR has the most negative surface. Although the net charge of *P. nautica* N_2OR dimer, −38, is similar to that of *A. cycloclastes* N_2OR dimer, −44, their electrostatic surfaces around the

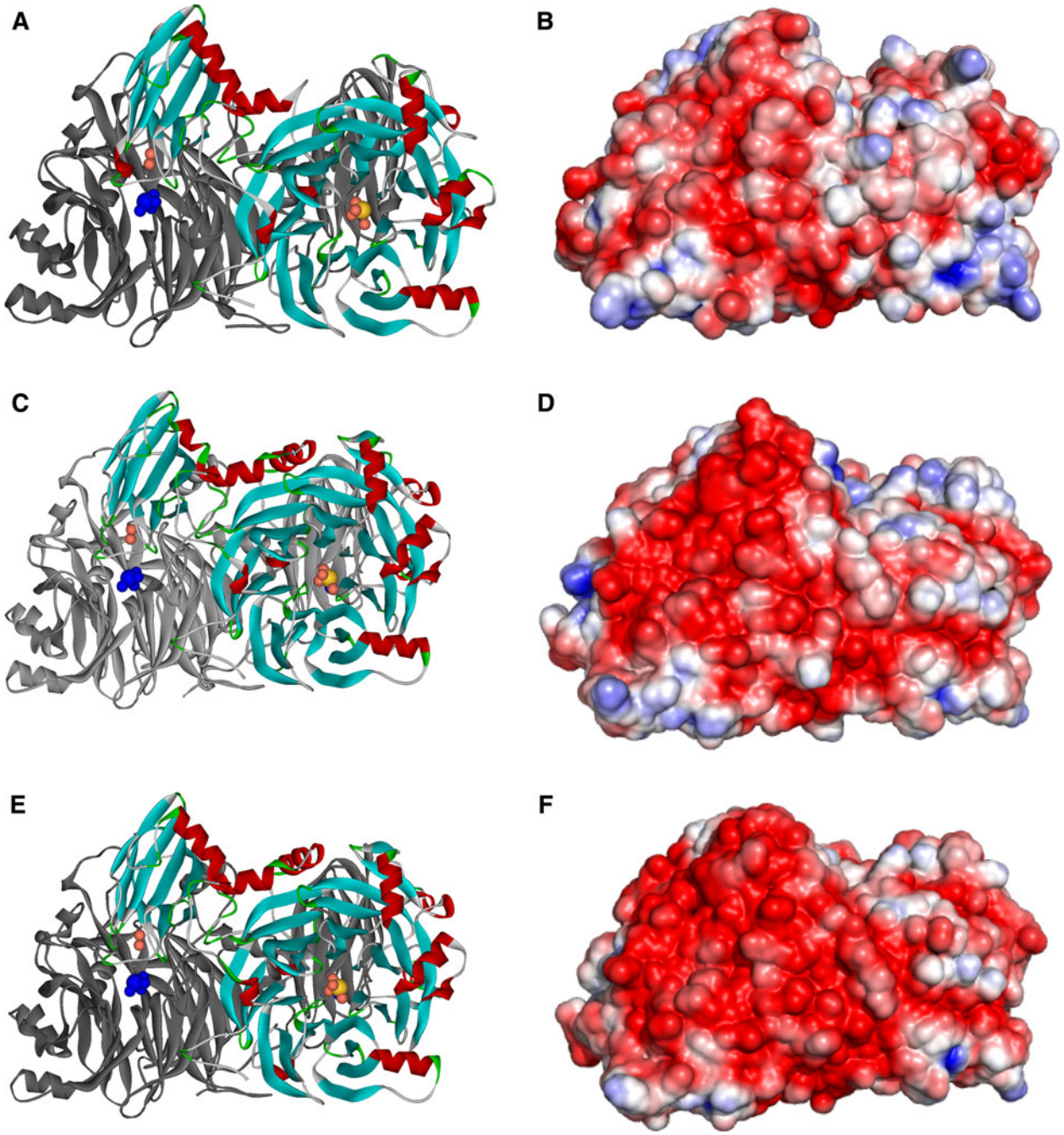

Fig. 1 Structures and electrostatic surface potentials of *Pseudomonas nautica* nitrous oxide reductase (N_2OR) (**a**, **b**), *Achromobacter cycloclastes* N_2OR (**c**, **d**), and *Paracoccus denitrificans* N_2OR (**e**, **f**). **a**, **c**, **e** The CuA and CuZ centers of the same monomer are colored *blue* and *light pink*, respectively. One of the N_2OR monomers is colored by secondary structure and the other is *gray*. The electrostatic surface potential is represented between −3 and 3 *kT/e* (**b**, **d**, **f**) (see "Methods"). The images were prepared using WebLab Viewer (Accelrys) (**a**, **c**, **e**) and PyMOL (**b**, **d**, **f**)

CuA center are quite different, with *A. cycloclastes* N_2OR being more negative and with a negative patch more similar to that of *P. denitrificans* N_2OR dimer (which has a global charge of −62).

As already suggested in previous studies [23, 43], the sequence alignment shows a high homology between *A. cycloclastes* N_2OR and *P. denitrificans* N_2OR, consisting of 89% identity, whereas *P. nautica* N_2OR has a lower sequence identity relative to the other two enzymes, with 59% identity with *P. denitrificans* N_2OR and 60% identity with *A. cycloclastes* N_2OR (Fig. S1). Moreover, the mapping of these conserved residues onto the structure of

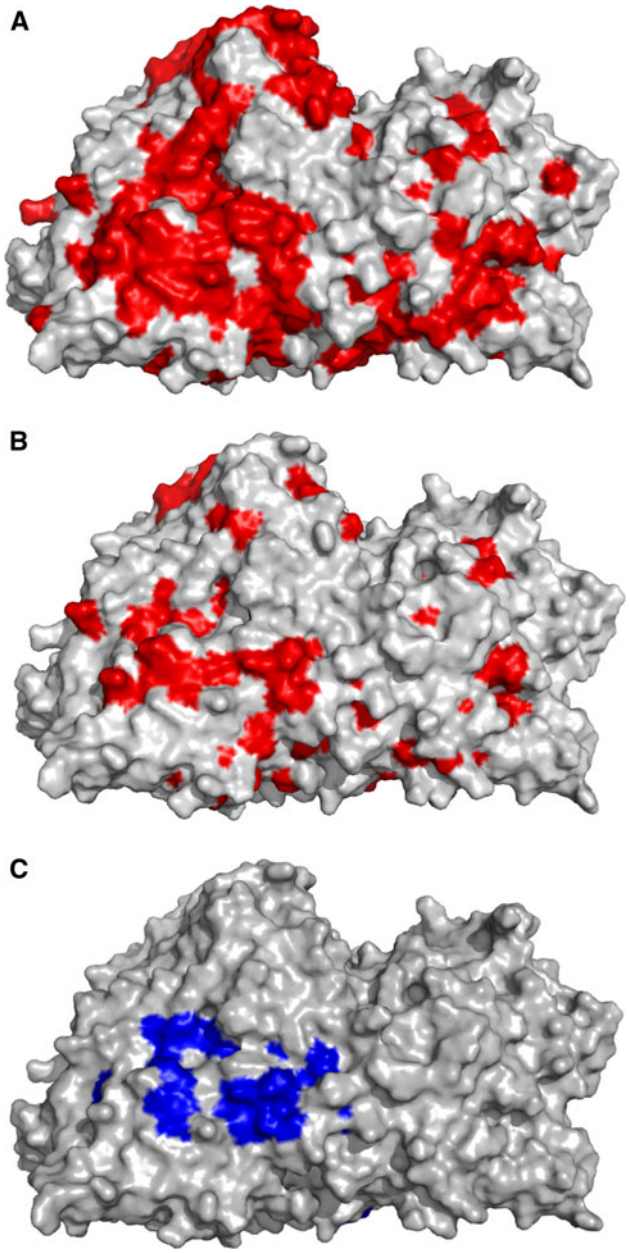

Fig. 2 **a** The conserved residues of *P. nautica*, *P. denitrificans*, and *A. cycloclastes* N_2ORs mapped onto the *P. nautica* N_2OR surface are colored *red*. **b** The conserved residues of *P. nautica*, *P. denitrificans*, *A. cycloclastes*, and *Wolinella succinogenes* N_2ORs mapped onto the *P. nautica* N_2OR surface are colored *red*. **c** Putative residues involved in the protein–protein interaction identified by WHISCY mapped onto the *P. nautica* N_2OR surface are colored *blue*. The images were prepared using WebLab Viewer (Accelrys)

P. nautica N_2OR identifies highly conserved regions, which include the interface between the two subunits, the residues coordinating the CuA and CuZ centers, and the surface near the CuA domain (Fig. 2a) [13].

The small electron carrier proteins that were used in the docking simulations are represented in Fig. 3. These proteins are either *c*-type cytochromes or type 1 copper proteins, and play the role of electron shuttles in the respiration and/or denitrification pathways.

Similarly to the analysis presented before for the N_2ORs used in this study, the global charges and the electrostatic surfaces of the small proteins were compared. Their global charges are quite different, ranging from positive, for mitochondrial cytochrome *c* (+8) and *P. nautica* cytochrome *c*-552 (+3), to neutral in the case of *A. cycloclastes* pseudoazurin and negative for *P. denitrificans* cytochrome *c*-550 (−2) and *P. panthotropus* pseudoazurin (−5).

However, even though they differ in their global charge, they share some common features. Indeed, all these small electron carrier proteins have a ring of positive residues around the proposed electron entry/exit point, which is located in a region composed mainly of hydrophobic residues (Fig. 3). The only exception is *P. nautica* cytochrome *c*-552, in which the number of charged residues around the exposed heme edge is clearly lower than in the other proteins (Fig. 3a). This cytochrome also differs from the other small proteins by being a homodimer, whereas the others are monomers (mitochondrial cytochrome *c* and *A. cycloclastes* pseudoazurin) or there is a monomer–dimer equilibrium dependent on the redox state (*P. denitrificans* and *P. panthotropus* cytochrome *c*-550 and pseudoazurin) [44].

In general, electrostatic interactions are proposed to be instrumental in the preorientation of the partners for the formation of the encounter complex and less important in the interface of the competent electron transfer complex. The presence of a large number of opposite charges in the interface of the complex can be detrimental for an efficient electron transfer, as one of the requirements to maintain the electron flow in a pathway is fast dissociation of the partners after electron transfer [4]. Indeed, it has been proposed that the reason for the presence, in the electron carriers, of salt bridges between the residues that compose the positive ring and nearby negatively charged residues is to attenuate the formation of strong electrostatic interactions at the interface of the electron transfer complex [44].

In the surface of the donor protein, besides this region of charged residues, there is a hydrophobic patch that surrounds the exposed entry/exit site of the electron [45]. This hydrophobic patch includes the exposed heme edge in the case of *c*-type cytochromes or an exposed histidine side chain that coordinates the copper center in the case of pseudoazurins [46, 47] (Fig. 3).

Another characteristic of the small electron transfer proteins is their "pseudo-specificity", which is the property that allows these small electron transfer proteins to function as electron donors to different enzymes in an electron transfer pathway, as the denitrification or aerobic electron transfer chain. In the case of pseudoazurin and cytochrome

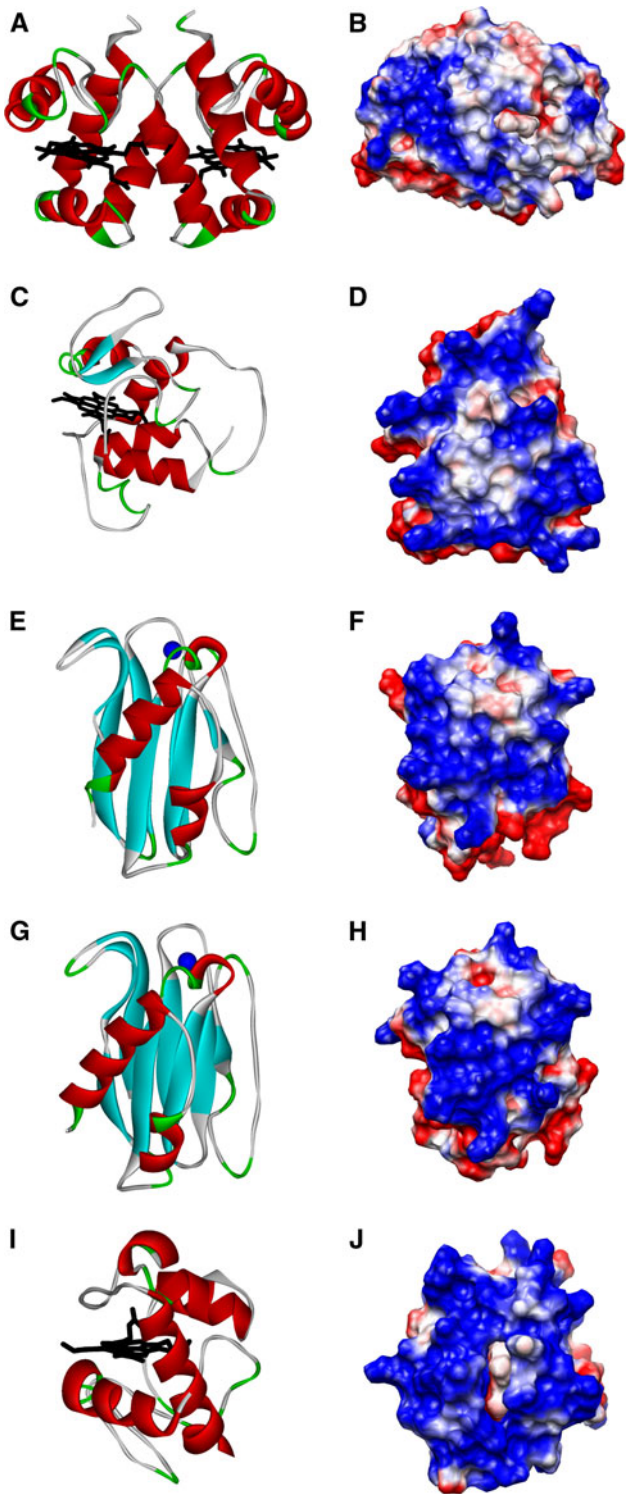

◀ **Fig. 3** Structures and electrostatic surface potentials of *P. nautica* cytochrome *c*-552 (**a**, **b**), *P. denitrificans* cytochrome *c*-550 (**c**, **d**), *Paracoccus panthotropus* pseudoazurin (**e**, **f**), *A. cycloclastes* pseudoazurin (**g**, **h**), and horse heart cytochrome *c* (**i**, **j**). **a**, **c**, **e**, **g**, **i** The backbone is colored according to secondary structure and the heme group is *colored black*, whereas the copper atom is *blue*. The electrostatic surface potential is represented between −4 and 4 *kT*/*e* (see "Methods"). The *images* on the *right* are rotated by 90° with respect to those on the *left*, so the proposed electron entry site is facing the reader. The images were prepared using the USCF Chimera program [35]

c-550 from *P. panthotropus*, it has been shown that they can both donate electrons to enzymes expressed in the periplasm of this organism when the bacterium is grown under microaerophilic or anaerobic conditions [48, 49].

In this study, it was also possible to assess the inter-species pseudo-specificity by determining whether some of the small electron carriers could potentially substitute the physiological donor of N_2OR in in vitro kinetic assays.

The comparison of the electrostatic surface of the small electron transfer proteins and of the enzymes from the different organisms shows that there are pairs of proteins that could be putative electron donors, whereas there are others that would be more difficult to conceive as redox partners. One of these examples is the interaction of mitochondrial cytochrome *c* and *P. nautica* N_2OR, which is actually not kinetically competent [18].

Molecular docking simulation

General analysis

A docking analysis of the complex formed between *A. cycloclastes* N_2OR, *P. denitrificans* N_2OR, and *P. nautica* N_2OR and the corresponding physiological or a group of nonphysiological electron donors was performed. In each case, the first stage of the BiGGER algorithm provided a set of 5,000 solutions chosen from all the possible orientations generated by rotating the small electron donor (probe) around the surface of each N_2OR (target) in steps of 1 Å and with a translation step of 15°. In the second stage, the top solutions ranked by global score and either hydrophobic score or electrostatic score, depending on the nature of the electron transfer complex (see "Methods" and vide infra), were analyzed taking into account the distance between the redox centers.

Although the primary sequence of *P. panthotropus* N_2OR is not known, it is expected to have a high identity with the *P. denitrificans* enzyme considering the high sequence identity that is found in other proteins from these two organisms (92 and 95% sequence identity for cytochrome *c*-550 and pseudoazurin, respectively). This high homology justifies not only the use of the *P. panthotropus* pseudoazurin structure in the docking studies, but also the use of the biochemical properties of *P. panthotropus* N_2OR. It was reported that the increase in ionic strength decreases the activity of *P. panthotropus* N_2OR in the presence of horse heart cytochrome *c*, which is an indication that the complex formed has an electrostatic nature [22]. The

electrostatic character has also been suggested for other electron transfer complexes involving pseudoazurin and/or cytochrome *c*-550 from these organisms, and *P. panthotropus* cytochrome *c* peroxidase [48] and *P. denitrificans* non-heme-iron hydroxylamine oxidase [50].

In the case of *P. nautica* N_2OR, the complex formed with cytochrome *c*-552, the physiological electron donor, is hydrophobic [18]. Although there is no report in the literature about the nature of the interaction of *A. cycloclastes* N_2OR with its electron donor, pseudoazurin, there are several studies that have shown that the *A. cycloclastes* copper-containing nitrite reductase and *A. cycloclastes* pseudoazurin form an electrostatic complex [51, 52]. Thus, we propose that the electron transfer complex between *A. cycloclastes* pseudoazurin and *A. cycloclastes* N_2OR has a similar nature.

Therefore, in the second stage of the docking, the putative complexes were analyzed taking into account the properties of these complexes as presenting an electrostatic or a hydrophobic character: the top 200 solutions were ranked by global, electrostatic, or hydrophobic score (their representations are shown in Figs. 4, S2–S4).

Previously, direct electron transfer studies have shown for *P. panthotropus* and *P. nautica* N_2OR that the small electron transfer proteins donate electrons directly to the binuclear CuA center of N_2OR [18, 22]. Therefore, the solutions were filtered using the condition that the distance between the redox centers, the CuA center and the iron ion of cytochrome *c*, or the copper ion of pseudoazurin, should be less than 20 Å, a condition required for an efficient electron transfer [15] (Table 1, and their representation is shown in Figs. S2–S4). This analysis is used to determine whether this docking program can be applied to discriminate between effective and noneffective electron donors.

In the case of *P. nautica* N_2OR, the complex with the electron donor cytochrome *c*-552 shows a higher number of putative effective electron transfer complexes for N_2OR compared with any of the other nonphysiological electron carrier proteins (Figs. 4, S4; Table 1). The number of solutions with an appropriate distance between the redox

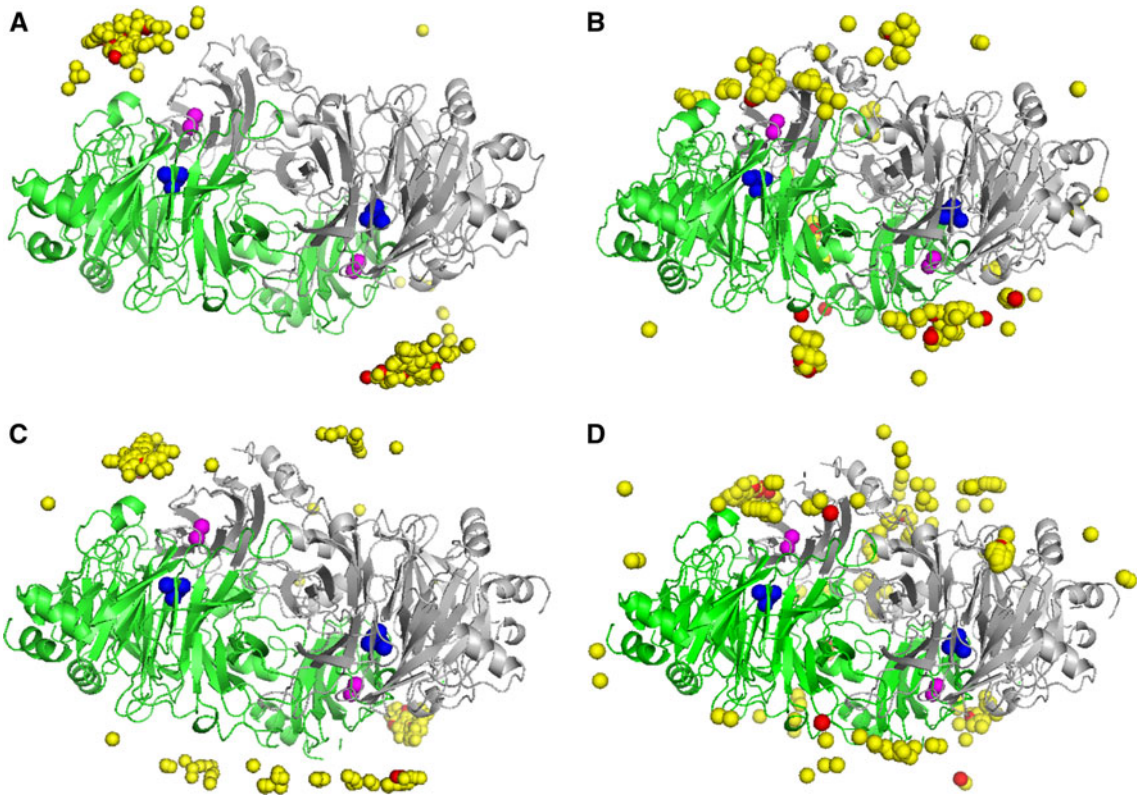

Fig. 4 The electron transfer complexes between N_2OR and its physiological electron donors. **a** The 200 top docking solutions ranked by hydrophobic score of *P. nautica* N_2OR with *P. nautica* cytochrome *c*-552. **b** The 200 top docking solutions ranked by electrostatic score of *A. cycloclastes* N_2OR with *A. cycloclastes* pseudoazurin. **c** The 200 top docking solutions ranked by electrostatic score of *P. denitrificans* N_2OR with *P. denitrificans* cytochrome *c*-550. **d** The 200 top docking solutions ranked by electrostatic score of *P. denitrificans* N_2OR with *P. panthotropus* pseudoazurin. The geometric center for cytochrome *c*-552, the copper atom for pseudoazurin, and the iron atom for cytochrome *c*-550 are represented as *yellow spheres*, with the top 20 solutions of these scores being represented as *red spheres*. N_2OR is shown as a backbone with one monomer colored *green* and the other colored *gray*, the two copper atoms of the CuA center are colored *magenta*, and the catalytic CuZ center is colored *blue*. The images were prepared using Chemera

Table 1 Analysis of the molecular dockings between nitrous oxide reductase (N_2OR) from different microorganisms and the electron donors performed using the BiGGER algorithm [7]

N_2OR source	Electron donor	Best 200 Gb $+d < 20$ Å[a]	Best 200 electrostatic $+d < 20$ Å[b]	Best 200 hydrophobic $+d < 20$ Å[c]
Pseudomonas nautica	***P. nautica* cytochrome *c*-552**	23	41	139
P. nautica	*P. denitrificans* cytochrome *c*-550	0	0	3
P. nautica	*Paracoccus panthotropus* pseudoazurin	0	4	4
P. nautica	*A. cycloclastes* pseudoazurin	1	4	8
P. nautica	Horse heart cytochrome *c*	0	0	0
Paracoccus denitrificans	*P. nautica* cytochrome *c*-552	4	34	66
P. denitrificans	***P. denitrificans* cytochrome *c*-550**	9	83	80
P. denitrificans	***P. panthotropus* pseudoazurin**	5	20	35
P. denitrificans	*A. cycloclastes* pseudoazurin	1	27	39
P. denitrificans	**Horse heart cytochrome *c***	12	92	108
Achromobacter cycloclastes	*P. nautica* cytochrome *c*-552	8	79	62
A. cycloclastes	*P. denitrificans* cytochrome *c*-550	12	126	42
A. cycloclastes	*P. panthotropus* pseudoazurin	9	26	40
A. cycloclastes	***A. cycloclastes* pseudoazurin**	6	85	55
A. cycloclastes	Horse heart cytochrome *c*	0	26	27
A. cycloclastes	**Bovine heart cytochrome *c***	1	44	37

The complexes that have been studied experimentally are highlighted in *bold*

[a] Number of solutions in the top 200 in the global score (*Gb*) ranking with a CuA–Fe/Cu distance shorter than 20 Å

[b] Number of solutions in the top 200 in the electrostatic ranking with a CuA–Fe/Cu distance shorter than 20 Å

[c] Number of solutions in the top 200 in the hydrophobic ranking with a CuA–Fe/Cu distance shorter than 20 Å

centers (heme–Fe and CuA) is maximum considering the hydrophobic score, as predicted taking into account the kinetic studies [18]. Moreover, it was shown that the positively charged horse heart cytochrome *c* was not able to donate electrons to *P. nautica* N_2OR, a result that corroborates the docking analysis, which does not present any solution with the appropriate orientation for electron transfer (Fig. S4.3).

On the other hand, this mitochondrial cytochrome was shown to be a competent electron donor to *P. denitrificans* N_2OR [22], and indeed the analysis of the docking simulation by the different scores gives rise to several top solutions in an orientation that is predicted to enable an effective electron transfer (Table 1). The number of these top orientations for electron transfer is similar whatever scoring function was used to rank them, even if the formation of the competent electron transfer complexes is proposed to be mainly driven by electrostatic forces.

The physiological electron donors of *P. denitrificans* N_2OR have long been established to be cytochrome *c*-550 and pseudoazurin [20, 21]. In the first case, the docking simulation gave several solutions in the top 200 of each ranking with a favorable orientation for electron transfer (Fig. 4c, d; Table 1). In the case of pseudoazurin, this protein has a lower number of probable solutions towards *P. denitrificans* N_2OR compared with cytochrome *c*-550 (vide infra).

Our results on *P. denitrificans* N_2OR are widely in agreement with a previous docking analysis performed with a different algorithm, FTDOCK [23], which strengthens both the use of the docking algorithm BiGGER and the method employed in this work for the analysis of the 5,000 solutions obtained from the ab initio soft-docking calculation.

In the last case study, the molecular docking simulation between *A. cycloclastes* N_2OR and its physiological electron donor, pseudoazurin, there are several putative docking solutions with a short distance between the redox center especially when the solution were ranked by the electrostatic score (Fig. 4b; Table 1).

The lower number of putative complexes obtained when pseudoazurins, from either *A. cycloclastes* or *P. panthotropus*, are used as probes can be attributed to the smaller size of the expected pseudoazurin surface interacting with N_2OR, when compared with that of the *c*-type cytochromes studied. Since there is a surface contact cutoff value below which BiGGER rejects all models, the number of "putatively competent" solutions that were rejected is expected to be higher in the docking calculations when pseudoazurin is a probe rather than in those in which cytochromes were used as probes.

It is interesting to note that the mitochondrial bovine heart cytochrome *c*, which was shown to be able to donate electrons to the CuA center of *A. cycloclastes* N_2OR, indeed behaves as a potential electron donor, with a larger number of putative solutions being found when the complexes were analyzed considering the interaction driven mainly by electrostatic forces (Fig.S2.1). Similarly, *P. denitrificans* cytochrome *c*-550 was also predicted, by BiGGER, to function as a putative electron donor to this enzyme (considering that the interaction has an electrostatic nature). This can be explained by the fact that the surfaces of these two electron shuttle proteins share a similar charge distribution (Fig. 3).

A summary of the analysis of the docking simulations combined with the previous experimental data is presented in Table S1.

Analysis of the top complexes

The interface-accessible area of the top solutions for each of the physiologic docking results was evaluated. These complexes have an interface area between 943 and 1,368 $Å^2$ (Table 2), which is typical for small, short-lived complexes following the criteria of Lo Conte et al. [3]. The docking models for the *P. nautica* cytochrome *c*-552–*P. nautica* N_2OR complex have a higher percentage of apolar residues in the interface area (with an average value of 79%), confirming the hydrophobic nature of the interaction. For *A. cycloclastes* N_2OR and *P. denitrificans* N_2OR complexes, the average values of apolar residues in the interface are 64 and 69%, respectively. This result shows that although the formation of these complexes is being driven by electrostatic forces, the area of contact

Table 2 Parameters of the top model complex obtained by docking simulation of N_2OR with the respective electron donor

Complex	ID	Gb (rank)	Elect. (rank)	Hydroph. (rank)	D^a (Å)	Coupling constant[b]	Pathway[c]	Interface area ($Å^2$)	Apolar residues[d] (%)
A. cycloclastes N_2OR–bovine heart cytochrome *c*	4142	1.9 (387)	−151.7 (56)	−6.0 (440)	15.7	2.8×10^{-5}	Fe–Ala554	1,366	66
A. cycloclastes N_2OR–*A. cycloclastes* pseudoazurin	3203	2.2 (102)	−91.5 (49)	−5.4 (918)	16.9	1.1×10^{-4}	Cu–Leu627	1,090	63
A. cycloclastes N_2OR–*A. cycloclastes* pseudoazurin	3167	2.1 (140)	−78.4 (162)	−6.6 (266)	18.9	9.4×10^{-6}	Cu–Leu627	1,115	64
P. denitrificans N_2OR–*P. panthotropus* pseudoazurin	3077	2.3 (71)	−22.7 (298)	−6.9 (150)	15.7	1.3×10^{-5}	Cu–Leu593	1,277	68
P. denitrificans N_2OR–*P. denitrificans* cytochrome *c*-550	4851	2.2 (62)	−101.4 (152)	−5.5 (1,385)	14.7	4.7×10^{-4}	Cu–His635	1,368	67
P. denitrificans N_2OR–horse heart cytochrome *c*	1712	1.9 (86)	−175.1 (121)	−6.7 (38)	15.5	2.8×10^{-4}	Fe–His635	1,289	70
P. nautica N_2OR–*P. nautica* cytochrome *c*-552	105	10.4 (35)	−22.7 (3,545)	−6.1 (13)	16.3	3.0×10^{-5}	Fe–Asp519	1,222	75
P. nautica N_2OR–*P. nautica* cytochrome *c*-552	579	9.2 (51)	−50.7 (312)	−7.0 (2)	17.5	3.0×10^{-5}	Fe–Gln497	1,211	79
P. nautica N_2OR–*P. nautica* cytochrome *c*-552	2181	10.4 (36)	−39.6 (1,118)	−4.8 (175)	17.9	2.1×10^{-6}	Fe–His566	943	84

Gb global score, *Elect.* electrostatic score, *Hydroph.* hydrophobic score, *rank* ranking of the solution with that ID in the respective score

[a] Distance between CuA in N_2OR and heme–Fe or Cu of cytochrome *c* or pseudoazurin, respectively

[b] The coupling constant is the value for the best electron transfer path from Cu or Fe atoms to CuA centers as analyzed using PATHWAYS

[c] The residue number is according to the primary sequence of N_2OR from each organism

[d] The percentage of apolar residues in the interface area of the complex

between the redox partners is hydrophobic, as expected in order to promote the electron transfer and provide more specificity to the complex [45].

The electron transfer complexes between *A. cycloclastes* N_2OR and *P. denitrificans* N_2OR and their electron donors can be ascribed to a docking scenario in which the electrostatic forces play the role of the long-range recognition between the donor and the acceptor and drive the formation of the complex; however, at short range, the hydrophobic patch also plays an important role in the fine-tuning of formation of the electron transfer complex.

Electron transfer pathway

To propose an electron pathway from the small electron donor protein to the CuA center and then to the catalytic center of N_2OR, the CuZ center, the top complexes for each of the docking calculations were further analyzed using the program PATHWAYS. The top complexes that were chosen had to obey the following criteria (Table 2):

- They had to be part of the top 200 solutions ranked by global score.
- They had to be part of the top solutions ranked by hydrophobic score for *P. nautica* N_2OR or by electrostatic score for *P. denitrificans* N_2OR and *A. cycloclastes* N_2OR docked complexes.
- The distance between the redox center of the small electron donor and the CuA center of N_2OR had be shorter than 20 Å.

Combining the analysis of the electron transfer pathway of the top complexes, we identified a conserved histidine (*A. cycloclastes* His625, *P. denitrificans* His635, and *P. nautica* His566) in the electron transfer pathway as the entry point in three of the complexes analyzed (Table 2), a leucine (*A. cycloclastes* Leu627, *P. denitrificans* Leu637, and *P. nautica* Leu568) in two complexes, and an aspartate (*A. cycloclastes* Asp578, *P. denitrificans* Asp588, and *P. nautica* Asp519), an alanine (*A. cycloclastes* Ala554, *P. denitrificans* Ala564, and *P. nautica* Ala495), a glutamine (*P. nautica* Gln497, which corresponds to *A. cycloclastes* Ser556 and *P. denitrificans* Ser566), and a leucine (*A. cycloclastes* Leu583 and *P. denitrificans* Leu593, which corresponds to *P. nautica* Val524) each just in one identified electron pathway (Table 2).

The sequence alignment shows that all these residues are conserved in the primary sequence of these N_2ORs, suggesting that these residues constitute a conserved region located near the CuA center that functions both as the binding site for the electron donor and as the electron entry point (Figs. 2a, 5a).

This conserved patch involved in complex formation and favorable electron transfer was also identified by the

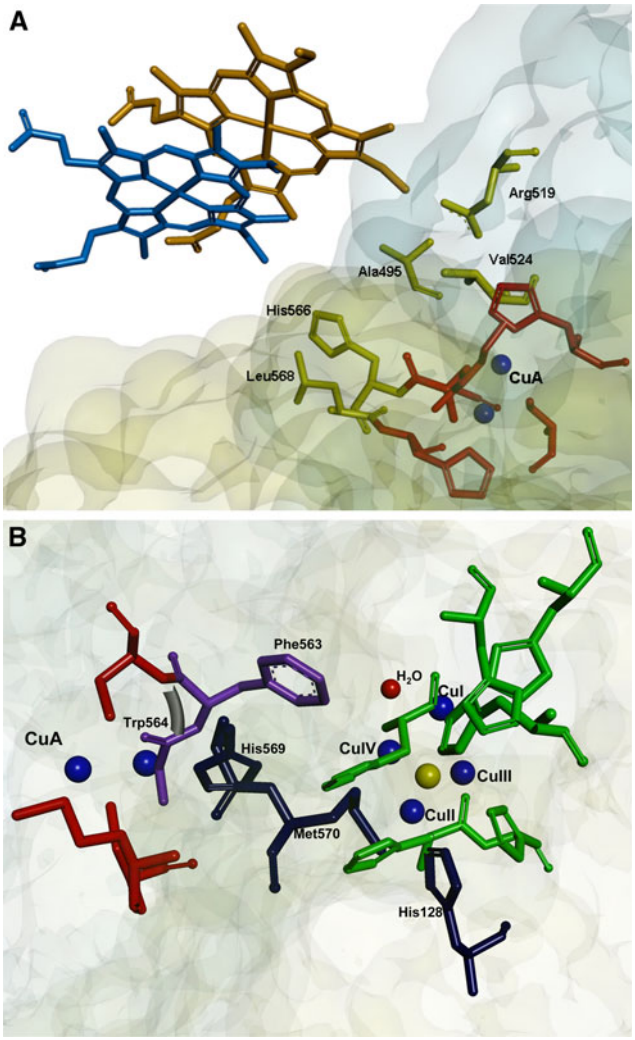

Fig. 5 Proposed electron transfer pathways in N_2OR. **a** The electron transfer pathway between cytochrome *c*-552 and the CuA center of *P. nautica* N_2OR is represented. Two possible orientations of cytochrome *c*-552 are shown (for clarity only the heme group of cytochrome *c*-552 is displayed). The residues involved in the electron transfer from the heme group to the CuA center (Ala495, Asp519, Val524, His566, Leu568) are represented in *yellow*. The ligands of the CuA center (His526, Cys561, Cys565, His569, Met572) are colored *red*. The copper atoms of the CuA center are represented as *blue spheres*. **b** Two different electron transfer pathways from the CuA center to the CuZ center are represented. The first route involves Trp563, which is a CuA ligand, and the neighbor Phe564 (Trp563 and Phe564 are represented in *purple*); the electron is then transferred to the oxygen of a water molecule or a hydroxyl group bound between CuI and CuIV of the CuZ center. An alternative route involves the electron transfer from the CuA center to His569, then to Met570, and subsequently to His128, which is a ligand of CuII of the CuZ center (His569, Met570, and His128 are represented in *blue*). The ligands of the CuZ center (His79, His80, His128, His270, His325, His376, His437) are represented in *green*. The copper atoms of CuZ are represented as *blue spheres*, and the sulfur atom in the CuZ center is represented in *yellow*. In **a** and **b** the surfaces of the two monomers of N_2OR are represented in *light green* and *light blue*, respectively

WHISCY program [40] as to constitute a putative surface involved in protein–protein interaction (Fig. 2c—only the *P. nautica* N_2OR surface is shown).

The coupling constants for this electron transfer pathway are between 4.7×10^{-4} and 2.1×10^{-6} (values calculated by PATHWAYS), in which the routes involving the surface conserved histidine (*A. cycloclastes* His625, *P. denitrificans* His635, and *P. nautica* His566) show the highest coupling constant (4.7×10^{-4} and 2.8×10^{-4} for *P. denitrificans* N_2OR complexes, Table 2).

The electron transfer pathway from the CuA center to the CuZ center was also analyzed with the PATHWAYS program. The most probable electron transfer pathway (with a coupling constant of 1.1×10^{-4}) implies that the electron is transferred from the CuA center to the tryptophan (*P. nautica* Trp563, *P. denitrificans* Trp632, *A. cycloclastes* Trp622) that is bound to the copper through the main-chain carbonyl group. Then, the electron is transferred to the neighbor phenylalanine (*P. nautica* Phe564, *P. denitrificans* Phe633, *A. cycloclastes* Phe623) and subsequently to the oxygen of a water molecule or a hydroxyl group, which is bound between two copper atoms of the CuZ center (CuI and CuIV) (Fig. 5b—pathway represented in purple), the proposed substrate binding site [53].

Although the catalytic mechanism of N_2OR is only partially known, theoretical calculations coupled with spectroscopic studies and enzymatic assays have shown that the most favorable state of the CuZ center to bind the substrate, N_2O, is the fully reduced state ($4Cu^+$) [54]. The electron transfer pathway identified above is in agreement with this mechanism, in which the reduction of the CuZ center occurs prior to substrate binding. After the first step of the reaction (the N–O bond cleavage), the CuZ center is proposed to be in the [$2Cu^{2+}$–$2Cu^+$] redox state and has to undergo two one-electron reductions to be again in the catalytically active redox state $4Cu^+$ [55]. During this reduction process, the oxygen bound to the CuZ center (between CuI and CuIV) has to be protonated to be released as a water molecule.

An alternative electron pathway (with a coupling constant of 4.3×10^{-5}) involves one of the histidine ligands of the CuA center (*P. nautica* His569, *P. denitrificans* His638, *A. cycloclastes* His628), then the neighbor methionine (*P. nautica* Met570, *P. denitrificans* Met639, *A. cycloclastes* Met629), and then transfer of the electron to the histidine (*P. nautica* His128, *P. denitrificans* His194, *A. cycloclastes* His184), which is a ligand of one of the copper atoms of the CuZ center (CuII) (Fig. 5b—pathway represented in blue). This electron transfer route is analogous to that proposed for the electron transfer from the CuA center to the heme *a* in cytochrome *c* oxidase [56].

Model structure for N_2OR from *W. succinogenes*

The N_2OR from *W. succinogenes* has an additional domain in its C-terminal with the canonical *c*-type-heme binding motif –CXXCH– [27, 28].

The structure of this protein has not yet been solved and can be proposed to resemble the electron transfer complex between an N_2OR and a *c*-type cytochrome. A protein sequence homology search shows that there are a few organisms that have this type of N_2OR, although none of these other enzymes have been isolated. These organisms are from the *Campylobacter*, *Sulfurimonas*, and *Denitrovibrio* genera, with the first two being host-associated organisms from the *Epsilonproteobacteria* group, as *W. succinogenes*.

The model structure of *W. succinogenes* N_2OR was built in two steps: first a model of the N-terminal N_2OR domain and of the C-terminal *c*-type-heme-containing domain were modeled, and afterwards these two domains were docked to obtain a model structure of the complete enzyme.

The N-terminal N_2OR domain, composed of the CuA and CuZ domains, shows sequence homology with all the N_2ORs with known structure, and the surface mapping of the conserved residues shows that there is a surface patch of conserved residues near the CuA center (Fig. 2b), a region also identified by WHISCY as involved in protein–protein interactions. However, since *P. nautica* N_2OR has the highest primary sequence identity with *W. succinogenes* N_2OR (34%), its structure (Protein Data Bank ID 1QNI) was used to model the N-terminal domain of *W. succinogenes* N_2OR using the PHYRE program.

As to the C-terminal domain, proposed to contain a *c*-type heme, different online programs and *c*-type cytochromes or *c*-type-heme-containing domains were used to model its structure (Fig. 6a) on the basis of sequence homology. In particular, four models were created using the structures of the following *c*-type-heme-containing templates: *Rhodothermus marinus* caa_3 cytochrome *c* domain (1W2L [57]), C-terminal domain of quinohemoprotein alcohol dehydrogenase from *Pseudomonas putida* HK5 (1KV9 [58]), the monohemic cytochrome c_2 from *Rhodopila globiformis* (1HRO [59]), and the monohemic cytochrome *c* from *R. marinus* (3CP5 [60]). The latter has the highest sequence identity (25%) and the model obtained gave the best results in the docking study. This model was obtained using SWISS-MODEL [42] (Fig. 6b), and shows that this domain has a surface with positive and negative patches (Fig. 6c, d), which is consistent with a solvent-exposed surface.

In the second stage, these two model structures, the N_2OR domain and the *c*-type cytochrome domain, were used as the target and probe, respectively, in a docking calculation. It is important to mention that there is a region

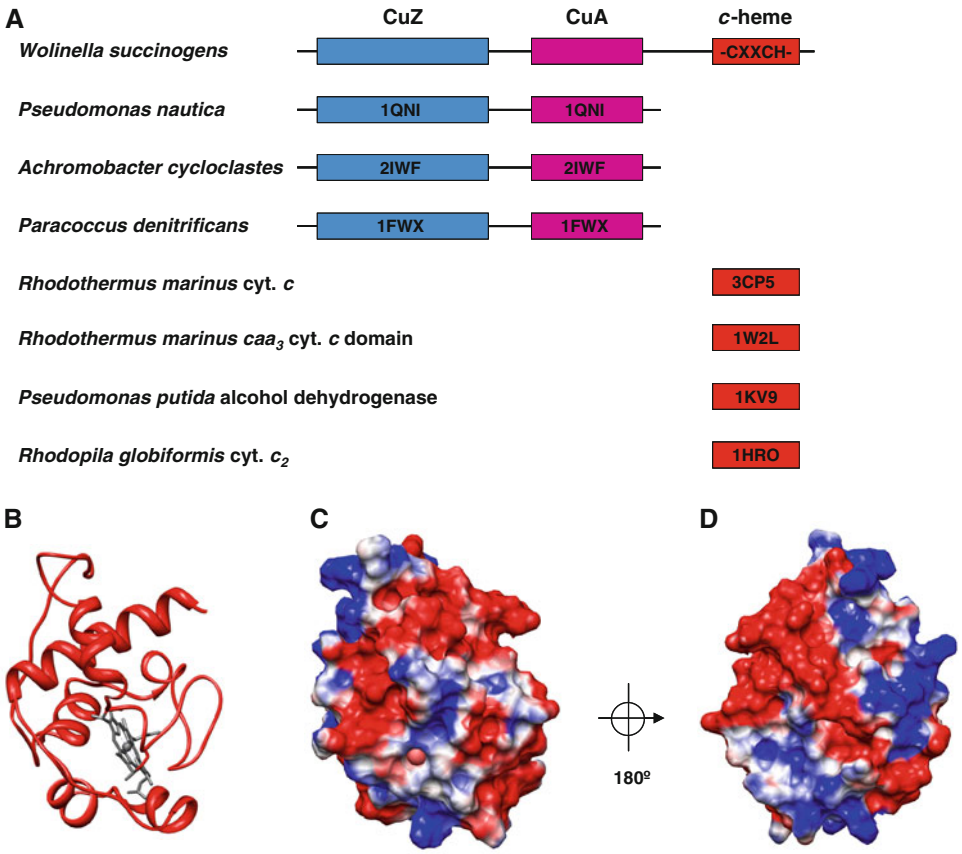

Fig. 6 The domains of *W. succinogenes* N_2OR and of other N_2ORs with known structure. The Protein Data Bank IDs of the structures used to model the C-terminal domain are shown in *red* (**a**). Structures 1QNI and 3CP5 were the ones that gave the highest scores for the N-terminal domain and the and C-terminal domain, respectively. The N-terminal domain of *W. succinogenes* N_2OR is composed of the CuZ domain (*blue*) and the CuA domain (*purple*), and the C-terminal domain containing the *c*-type-heme binding motif is represented as a *red box*. The model of the C-terminal domain of *W. succinogenes* N_2OR is shown as a backbone (**b**) and its surface is shown colored by electrostatic potential (**c**, **d**). The electrostatic surface potential is represented between −4 and 4 *kT/e* (calculated as described in "Methods" for the small *c*-type cytochromes). The images were prepared using the USCF Chimera program [35]

(100 residues) between the N-terminal N_2OR-type domain and the C-terminal *c*-type-heme-containing domain which has very low homology with known protein structures. For this reason we cannot provide a realistic linker connecting the N- and the C-terminal domains. However, an acceptable docking geometry can be selected taking into account that for an effective electron transfer the distance between the CuA center and the heme iron of the heme in the C-terminal domain should be less than 20 Å.

The analysis of the docking results shows that there is one solution that fulfils this criterion, providing us with a possible model structure of *W. succinogenes* N_2OR (Fig. 7a).

The PATHWAYS analysis of these two models determined a distance of 17.8 and 18.8 Å between the heme iron and the CuA center, with Arg557 and Cys627 in the N_2OR domain as the key residues for the electron entry. Arg557 corresponds to the conserved alanine proposed to be part of the electron transfer pathway in the other N_2OR complexes studied (*A. cycloclastes* Ala554, *P. denitrificans* Ala564, and *P. nautica* Ala495), and Cys627 is the neighboring residue of Ser628, which corresponds to the conserved histidine residue proposed before to be the electron entry point (*A. cycloclastes* His625, *P. denitrificans* His635, and *P. nautica* His566).

The analysis of the electrostatic surface of the cytochrome *c* domain modeled on the basis of *R. marinus* cytochrome *c* reveals a prevalently charged surface, which means that this domain might not be tightly bound to the N_2OR domain.

Therefore, a mechanism for the electron transfer reaction in *W. succinogenes* N_2OR can be proposed in which the *c*-type-heme-containing domain can assume different orientations. In particular, the *W. succinogenes* N_2OR might present an "open conformation" to allow the *c*-type-heme-containing domain to receive electrons from an electron donor (Fig. 7b), which is proposed to be a periplasmic cytochrome *c* [28]. After the reduction of the *c*-type-heme-containing domain, the enzyme can rearrange into a "close conformation" in which the heme group assumes the appropriate orientation to donate electrons to the CuA center (Fig. 7b).

Conclusion

In conclusion, this docking study predicted the interacting geometries between N_2OR and its physiological electron donors. These models are corroborated by experimental data and in the case of *P. denitrificans* N_2OR are in agreement with the previously proposed electron transfer complexes [23].

A set of well conserved residues were identified as being involved in the electron transfer pathway, suggesting the

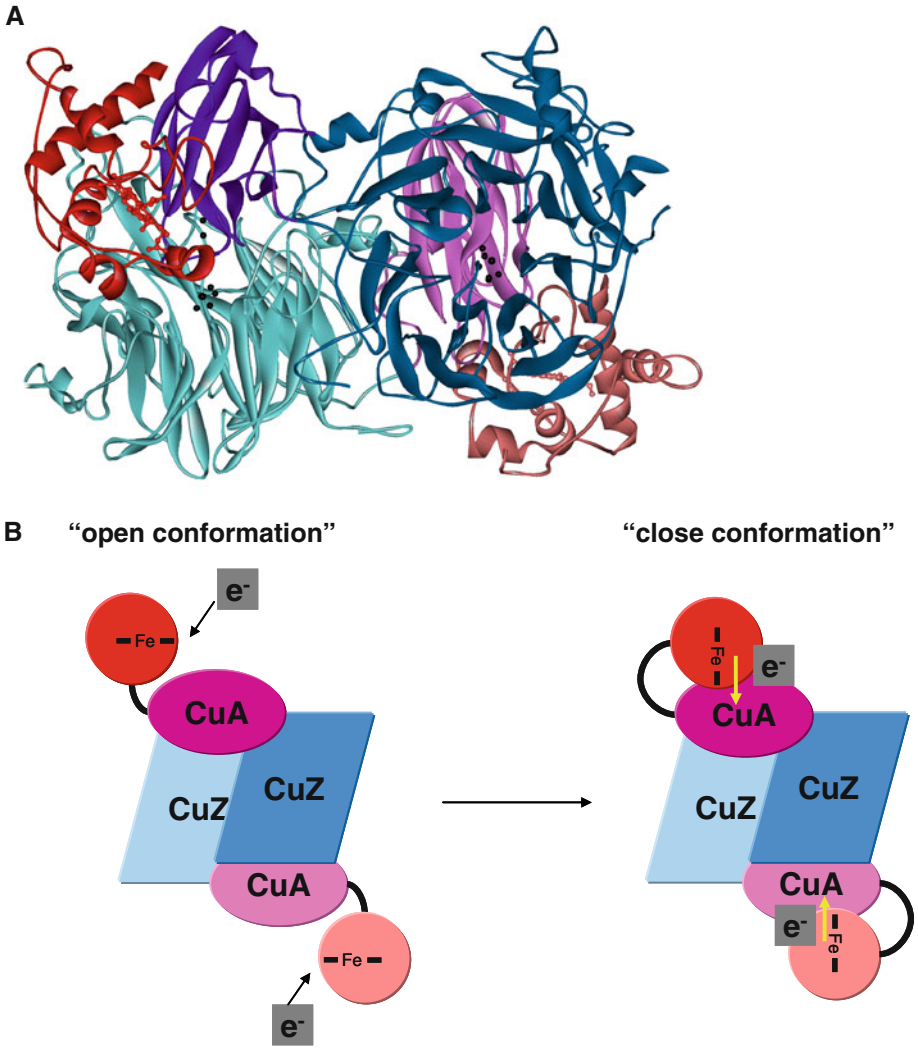

Fig. 7 **a** Proposed model for the *W. succinogenes* N_2OR, which has an additional C-terminal domain with a *c*-type heme. The C-terminal domain (*red* or *pink*) is shown to interact with the surface of the N_2OR domain surrounding the CuA domain, the proposed entry site for the electron. The two copper atoms of the CuA center and the catalytic CuZ center are colored *black* and the CuA and CuZ domains of N_2OR are colored *purple* and *blue*, respectively. **b** Proposed scheme for the electron transfer mechanism in *W. succinogenes* N_2OR. The CuA and CuZ domains are represented in *purple* and *blue*, respectively, and the cytochrome *c* domain is *red* and *pink*. To receive the electron from the electron donor, *W. succinogenes* N_2OR is in an "open conformation"; to transfer an electron from the *c*-type heme domain to the CuA domain, the enzyme rearranges to a "close conformation"

presence of a specific region in both the donor and the acceptor proteins that enables the molecular recognition, formation of the encounter complex, and efficient electron transfer. However, it was not possible to identify a single electron transfer route, and instead a patch of surface residues was identified as being instrumental for partner recognition and complex formation, and involved in the electron transfer pathway.

Moreover, the electron transfer pathway between the CuA center and the CuZ center was investigated, suggesting two alternative routes for the reduction of the catalytic center, which agree with the accepted catalytic mechanism of this enzyme: full reduction of the CuZ center is required prior to N_2O binding.

A model structure for the *W. succinogenes* N_2OR, which has an additional C-terminal domain containing a *c*-type heme, was proposed. This model presents the heme iron at a distance of 18–19 Å from the CuA center of the N_2OR domain, forming a putative efficient electron route.

This work shows that BiGGER algorithm can be used to identify putative electron transfer partners that could be used as artificial electron donors in in vitro assays, or to propose the physiologic redox partner of an enzyme when there are several candidates in the same organism. The information presented here and the model structures can also be used as starting points for mutagenesis studies to unambiguously identify residues that are involved in electron transfer and/or partner recognition.

Acknowledgments This research was supported by Fundação para a Ciência e Tecnologia grants PTDC/QUI/64638/2006 (to I.M.) and SFRH/BD/30414/2006 (to S.D.).

References

1. Zumft WG (1997) Microbiol Mol Biol Rev 61:533–616
2. Tavares P, Pereira AS, Moura JJG, Moura I (2006) J Inorg Biochem 100:2087–2100

3. Lo Conte L, Chothia C, Janin J (1999) J Mol Biol 285:2177–2198
4. Prudencio M, Ubbink M (2004) J Mol Recognit 17:524–539
5. Sukumar N, Chen Z-w, Ferrari D, Merli A, Rossi GL, Bellamy HD, Chistoserdov A, Davidson VL, Mathews FS (2006) Biochemistry 45:13500–13510
6. Moreira IS, Fernandes PA, Ramos MJ (2010) J Comput Chem 31:317–342
7. Palma PN, Krippahl L, Wampler JE, Moura JJG (2000) Proteins 39:372–384
8. Xu X, Schurmann P, Chung J, Hass M, Kim S, Hirasawa M, Tripathy J, Knaff D, Ubbink M (2009) J Am Chem Soc 131:17576–17582
9. Fantuzzi A, Meharenna YT, Briscoe PB, Guerlesquin F, Sadeghi SJ, Gilardi G (2009) Biochim Biophys Acta 1787:234–241
10. Almeida RM, Pauleta SR, Moura I, Moura JJG (2009) J Inorg Biochem 103:1245–1253
11. Zumft WG, Kroneck PM (2007) Adv Microb Physiol 52:107–227
12. Brown K, Tegoni M, Prudencio M, Pereira AS, Besson S, Moura JJG, Moura I, Cambillau C (2000) Nat Struct Biol 7:191–195
13. Haltia T, Brown K, Tegoni M, Cambillau C, Saraste M, Mattila K, Djinovic-Carugo K (2003) Biochem J 369:77–88
14. Paraskevopoulos K, Antonyuk SV, Sawers RG, Eady RR, Hasnain SS (2006) J Mol Biol 362:55–65
15. Winkler JR (2000) Curr Opin Chem Biol 4:192–198
16. Witt H, Malatesta F, Nicoletti F, Brunori M, Ludwig B (1998) J Biol Chem 273:5132–5136
17. Maneg O, Ludwig B, Malatesta F (2003) J Biol Chem 278:46734–46740
18. Dell'Acqua S, Pauleta SR, Monzani E, Pereira AS, Casella L, Moura JJG, Moura I (2008) Biochemistry 47:10852–10862
19. Berks BC, Baratta D, Richardson J, Ferguson SJ (1993) Eur J Biochem 212:467–476
20. Moir JWB, Ferguson SJ (1994) Microbiology 140:389–397
21. Koutny M, Kucera I, Tesarik R, Turanek J, Van Spanning RJ (1999) FEBS Lett 448:157–159
22. Rasmussen T, Brittain T, Berks BC, Watmough NJ, Thomson AJ (2005) Dalton Trans 3501–3506
23. Mattila K, Haltia T (2005) Proteins 59:708–722
24. Fujita K, Ijima F, Obara Y, Hirasawa M, Brown DE, Kohzuma T, Dooley DM (2009) J Biol Inorg Chem 14(Suppl 1):S11–S20
25. Liu MY, Liu MC, Payne WJ, Legall J (1986) J Bacteriol 166:604–608
26. Fujita K, Chan JM, Bollinger JA, Alvarez ML, Dooley DM (2007) J Inorg Biochem 101:1836–1844
27. Teraguchi S, Hollocher TC (1989) J Biol Chem 264:1972–1979
28. Zhang CS, Hollocher TC (1993) Biochim Biophys Acta 1142:253–261
29. Brown K, Nurizzo D, Besson S, Shepard W, Moura J, Moura I, Tegoni M, Cambillau C (1999) J Mol Biol 289:1017–1028
30. Benning MM, Meyer TE, Holden HM (1994) Arch Biochem Biophys 310:460–466
31. Najmudin S, Pauleta SR, Moura I, Romao MJ (2010) Acta Crystallogr Sect F Struct Biol Cryst Commun 66:627–635
32. Inoue T, Nishio N, Suzuki S, Kataoka K, Kohzuma T, Kai Y (1999) J Biol Chem 274:17845–17852
33. Bushnell GW, Louie GV, Brayer GD (1990) J Mol Biol 214:585–595
34. Mirkin N, Jaconcic J, Stojanoff V, Moreno A (2008) Proteins 70:83–92
35. Pettersen EF, Goddard TD, Huang CC, Couch GS, Greenblatt DM, Meng EC, Ferrin TE (2004) J Comput Chem 25:1605–1612
36. Betts JN, Beratan DN, Onuchic JN (1992) J Am Chem Soc 114:4043–4046
37. Regan JJ, Risser SM, Beratan DN, Onuchic JN (1993) J Phys Chem 97:13083–13088
38. Onuchic JN, Beratan DN, Winkler JR, Gray HB (1992) Annu Rev Biophys Biomol Struct 21:349–377
39. Thompson JD, Higgins DG, Gibson TJ (1994) Nucleic Acids Res 22:4673–4680
40. de Vries SJ, van Dijk ADJ, Bonvin AMJJ (2006) Proteins 63:479–489
41. Kelley LA, Sternberg MJ (2009) Nat Protoc 4:363–371
42. Bordoli L, Kiefer F, Arnold K, Benkert P, Battey J, Schwede T (2008) Nat Protoc 4:1–13
43. Prudencio M, Pereira AS, Tavares P, Besson S, Cabrito I, Brown K, Samyn B, Devreese B, Van Beeumen J, Rusnak F, Fauque G, Moura JJG, Tegoni M, Cambillau C, Moura I (2000) Biochemistry 39:3899–3907
44. Pauleta SR, Guerlesquin F, Goodhew CF, Devreese B, Van Beeumen J, Pereira AS, Moura I, Pettigrew GW (2004) Biochemistry 43:11214–11225
45. Williams PA, Fulop V, Leung YC, Chan C, Moir JW, Howlett G, Ferguson SJ, Radford SE, Hajdu J (1995) Nat Struct Biol 2:975–982
46. Kukimoto M, Nishiyama M, Ohnuki T, Turley S, Adman ET, Horinouchi S, Beppu T (1995) Protein Eng 8:153–158
47. Pelletier H, Kraut J (1992) Science 258:1748–1755
48. Pauleta SR, Cooper A, Nutley M, Errington N, Harding S, Guerlesquin F, Goodhew CF, Moura I, Moura JJG, Pettigrew GW (2004) Biochemistry 43:14566–14576
49. Pearson IV, Page MD, van Spanning RJM, Ferguson SJ (2003) J Bacteriol 185:6308–6315
50. Moir JW, Wehrfritz JM, Spiro S, Richardson DJ (1996) Biochem J 319:823–827
51. Kukimoto M, Nishiyama M, Tanokura M, Adman ET, Horinouchi S (1996) J Biol Chem 271:13680–13683
52. Kataoka K, Yamaguchi K, Kobayashi M, Mori T, Bokui N, Suzuki S (2004) J Biol Chem 279:53374–53378
53. Ghosh S, Gorelsky SI, Chen P, Cabrito I, Moura JJ, Moura I, Solomon EI (2003) J Am Chem Soc 125:15708–15709
54. Dell'Acqua S, Pauleta SR, Moura I, Moura JJG (2011) J Biol Inorg Chem 16:183–194
55. Gorelsky SI, Ghosh S, Solomon EI (2006) J Am Chem Soc 128:278–290
56. Wang K, Geren L, Zhen Y, Ma L, Ferguson-Miller S, Durham B, Millett F (2002) Biochemistry 41:2298–2304
57. Srinivasan V, Rajendran C, Sousa FL, Melo AM, Saraiva LM, Pereira MM, Santana M, Teixeira M, Michel H (2005) J Mol Biol 345:1047–1057
58. Chen ZW, Matsushita K, Yamashita T, Fujii TA, Toyama H, Adachi O, Bellamy HD, Mathews FS (2002) Structure 10:837–849
59. Benning MM, Meyer TE, Holden HM (1996) Arch Biochem Biophys 333:338–348
60. Stelter M, Melo AM, Pereira MM, Gomes CM, Hreggvidsson GO, Hjorleifsdottir S, Saraiva LM, Teixeira M, Archer M (2008) Biochemistry 47:11953–11963